Doubled Thrust by Boundary Layer Control in Scramjet Engines in Mach 4 and 6

Tohru Mitani, Noboru Sakuranaka, Sadatake Tomioka, Kan Kobayashi and Takeshi Kanda

Japan Aerospace Exploration Agency, Space Propulsion Research Center
1 Kimigaya, Koganesazawa, Kakuda, Miyagi 989-1525, Japan
Phone: +81-224-68-3640, Fax: +81-224-68-3206, E-mail: mitani.tohru@jaxa.jp

key words: scramjet, boundary layer bleed, two-staged combustion

Abstract

Boundary layer ingestion in airframe-integrated scramjet engines causes engine stall ("engine unstart" hereafter) and restricts engine performance. To improve the unstart characteristics in engines, boundary layer bleed and a two-staged injection of fuel were examined in Mach 4 and Mach 6 engine tests. A boundary layer bleed system consisting of a porous plate, an air coolers, a metering orifice and an ON/OFF valve, was designed for each of the engines. First, a method to determine bleed rate requirements was developed. Porous plates were designed to suck air out of the Mach 4 engine at a rate of 200 g/s and out of the Mach 6 engine at a rate of 30 g/s. Air coolers were then optimized based on the bleed airflow rates. The exhaust air temperature could be cooled below 600 K in the porous plates and the compact air coolers. The Mach 4 engine tests showed that a small bleed rate of 3% doubled the engine operating range and thrust. With the assistance of two-staged fuel injection of H2, the engine operating range was extended to Φ0.95 and the maximum thrust was tripled to 2560 N. The Mach 6 tests showed that a bleed of 30 g/s (0.6% of captured air in the engine) extended the start limit from Φ0.48 to Φ1 to deliver a maximum thrust of 2460 N.

Introduction

Airframe-integrated scramjet engines swallow the boundary layer developed on airframes of space planes. This ingestion promotes boundary layer separation in the engine and causes engine stall in combustion tests ("engine unstart" because of loss of thrust). As a result, maximum fuel supply rates and thrust are limited. Tests of our H_2-fueled scramjet engines have previously shown that the limit equivalence ratios (Φ^*) at the engine unstart were 0.3 at Mach 4 and about 0.5 at Mach 6 and 8 flight conditions.[1] The Φ^* was greatly changed by exclusion of the boundary layers, in which the engine was moved into the nozzle core region.[2] In scramjet engines, however, the exclusion of the boundary layer by diverters is unrealistic because of severe aerodynamic heating and large installation drag.

Therefore, other methods for suppressing boundary layer separation are required. Methods of boundary layer control in subsonic flows are well summarized in Ref. 3. Some data on bleed hole arrangements and discharge coefficients have also been reported,[4-8] although there have been few reports on their effects of engine inlets, especially in supersonic engine performance.[9-11] Yanta et al.[10] conducted a wind tunnel test with a bleed rate of 1.5% in a M4 ramp-compression inlet. Shimura et al.[11] reported the effect of engine unstart prevention in 1/5-subscaled models of our scramjet engines. However, no quantitative discussion on prevention of unstart have been reported.

To improve the unstart characteristics in our engines, boundary layer bleed and two-staged injection of fuel were examined in M4[12] and M6 engine tests[13]. Figure 1 is a side view of our engine, where the lower side is the topwall and the upper side is the cowl of the engine. Supersonic flow, accompanying the boundary layer, approaches the engine from the left. The thick boundary layer on the topwall of the engine is bled out through a porous plate. Two-staged injection is tested by adding a second fuel orifice row downstream of the combustor. This distributed injection may moderate the pressure rise due to heat release in the combustor and consequently prevent engine unstart at higher fuel injection rates. Details of the engine test and results have been previously reported.[12, 13] Those engine test data were compared with theoretical values and quantified as achievement factors.[14]

In this paper, details of the boundary layer bleed

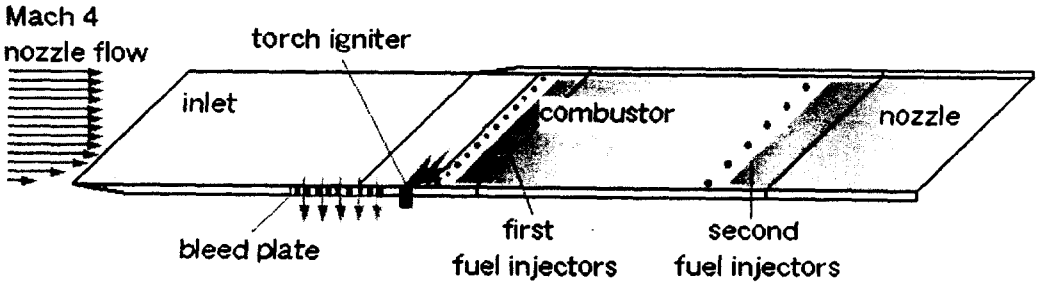

Figure 1 Boundary layer ingestion, boundary layer bleed and two-staged injection of H2 in the M4 engine

Table 1 Test conditions and thrust performance measured in engine tests

	M1	P0	T0	d1	ε	ηc	Ma	M)H2	Φ	ΔFexp	Dint	Fnet	Isp)f
unit	-	MPa	K	mm	-	-	kg/s	g/s	-	N	N	N	km/s
M4 without strut	3.4	0.86	870	11.7	2.86	0.72	6.70	195	0.30	1200	570	630	10.8
3%-bleed	3.4	0.86	870	11.7	2.86	0.72	6.50	195	0.66	2300	700	1400	12.4
3%-bleed & staged H2	3.4	0.86	870	11.7	2.86	0.72	6.50	195	0.95	2560	700	1860	10.0
M6 with 5/5H-strut	5.3	4.8	1500	19.7	5.00	0.80	5.00	145	0.48	1620	780	840	12.0
0.6%-bleed	5.3	4.8	1500	19.7	5.00	0.80	5.00	145	1.00	2460	780	1680	11.6

are described and the improvement of engine performance by bleed and two-stage injection is reviewed.

Engine Geometry and Test Conditions[1]

Our side-compression-type engine shown in Fig. 1 is rectangular and consists of a cowl, a top wall and two sidewalls. The entrance and the exit of the engine are 200 mm wide, 250 mm high and 2.1 m in length. The inlet has a wedge with a 6-degree half-angle and a swept-back angle of 45 degrees to deflect the airstream for suitable spillage required in starting. The geometrical contraction ratio (ε) is 2.86 without struts for the M4 tests and a higher value of ε = 5 with installation of a 30-mm-thick strut for the M6 tests. The engine is mounted upside down on a force balance as shown in Fig.1. The test conditions and engine performances are summarized in Table 1, where the inlet Mach number (M_1), the geometric contraction ratio (ε) and the air capture ratio (η_c) are shown. The lower M1, compared with the flight Mach numbers, represents the engine inlet condition behind the bow shock of vehicles. The 99%-thickness of boundary layers are denoted by d_1 in Table 1.

In the M4 tests, the mass rate (Ma in kg/s) of air flowing in the inlet is 6.7 kg/s from η_c. As shown in Table 1 the airflow rate in the combustor, however, decreases to 6.5 kg/s due to the boundary layer bleed. The Ma with the strut is 5.0 kg/s with boundary layer ingestion in the M6 condition. The bleed rate in the M6 test is so small that the Ma to the combustor is unchanged (5.0 kg/s). Hydrogen (H_2) fuel was injected perpendicular to the sidewall from 24 sonic orifices (1.5 mm in diameter) located 30 mm-downstream of backward-facing steps in the combustor. The stoichiometric H_2 rate in Table 1 was determined by the airflow rates and found to be from 195 g/s (M4-strutless engine) to 145 g/s (M6-engine with the 30-mm-thick strut). In some M4 tests, two-staged injection of H_2 was examined to improve the thrust performance where the additional H_2 was injected 558 mm downstream of the combustor step.

The limit equivalence ratio (Φ^*) in engines without boundary controls was found to be 0.3 in the engine with a strut at the M4 conditions and 0.48 in the engine with a strut at the M6. To extend the Φ^* up to Φ = 1 and increase the thrust gain, boundary layer bleed was tested. Thrust increment by combustion (ΔF) is defined as the difference in force readings with and without fuel supplies. The thrust increment should exceed engine internal drag (Dint), which is a measure of irreversible, intrinsic losses to produce ΔF. In Table 1, net thrust (ΔFnet) is obtained by subtracting Dint from ΔF. Dividing ΔF by fuel flow rate yields fuel-specific impulse.

Design of Boundary-Layer Bleed Systems

Bleed Rates to Prevent "Engine Unstart"

The boundary layer is thickest on the topwall because of boundary layer ingestion. The bleed rates on the topwall were determined by a simplified boundary layer consideration. Figure 2 shows maximum pressure rises observed in our engine tests under M4 to M8 conditions, in which P1 denotes pressure in the isolator without combustion and P2 is a maximum pressure just before unstart due to combustion. The engines fell into unstart condition when the pressure in the isolators exceeded the critical values. Since engine unstart is triggered by boundary layer separation in the isolators, the critical pressure ratios can be correlated with Mach numbers there. There are three lines in Fig. 2. When the adverse pressure is greater than the lines, the boundary layer may separate in the isolators. The broken line denotes the thermal choke limit given by Eq. (1), where γ (= 1.4) denotes the specific heat ratio. The line specified by Eq. (2) is the empirical limit of boundary layer separation proposed by Holden[15] in which cf is the wall friction coefficient. In our engine tests to date, many data on critical pressure rises under engine combustion conditions have been accumulated. The data under conditions of boundary layer ingestion are distributed around the line given by Eq. (3). In Eq. (3), a coefficient of 0.3 was proposed for two-dimensional separation by Korkegi.[16] However, Fig. 2 shows that a smaller value of 0.25 gives a better correlation with our three-demensional separation data obtained in engine tests.

$$P_2/P_1 = \left(1+\gamma M^2\right)/(1+\gamma) \qquad (1)$$

$$P_2/P_1 = 1 + 60 \cdot c_f \cdot M^3 \quad \text{with } cf = 0.002 \qquad (2)$$

$$P_2/P_1 = 1 + 0.25 \cdot M^2 \qquad (3)$$

Because the isolator Mach number can be calculated by one-dimensional analysis, the critical pressure rise ΔP is obtained from Eq. (2). When a boundary layer is subjected to ΔP, the separation can be prevented by removal of the bottom layer with local dynamic

pressure lower than ΔP. Note that pressure rise assuming a normal shockwave yields no significant difference since Mach number in the bottom layer is small. The 1/7th power law for velocity distribution in supersonic boundary layers showed that the bottom layer with a local Mach number less than a critical value should be sucked out. The critical Mach number was found to be approximately M* = 1.6 for the M4 and M6 engines. This method yields that the critical bleed rates are 120 g/s (M4) and 130 g/s (M6). Bleed devices were designed to bleed a target flow rate of 200 g/s in our engine test conditions.

Figure 3 shows shockwave patterns and arrangements of the bleed plate, where the upper half being for the M4 condition and the lower half for the M6 condition. The streamwise locations are measured from the leading edge of the sidewall. The exit of the inlet is at x = 617 mm and the backward facing step in the combustor is at x = 817 mm. A constant area section with a 70-mm-wide isolator is stationed at 617 mm < x < 817 mm. The two circles in Fig. 3 just upstream of the step represent the torch ignitors in the M4 and M6 tests.

An oblique shockwave is generated at the leading edge of the sidewall, reflected back at the center (x = 242 mm) and impinges at x = 408 mm on the sidewall. The shockwave reflection raise the wall pressure near the exit of the inlet. Similarly, the shockwave in the M6 condition is reflected back at x = 585 mm on the sidewall and another shockwave is generated at the leading edge of the strut (x = 475 mm). Thus, the region near the exit of the inlet suffers the most severe, adverse pressure. Therefore, the starting points of bleed were chosen to be x = 510 mm for the M4 and 540 mm for the M6 engines in order to bleed the boundary layer developed in the inlet. The pressure rise due to combustion moves upstream from the combustor step located at x = 817 with increasing fuel rate. The terminal point of the porous plates was set at x = 704 mm to prevent boundary layer separation in the inlet by combustion.

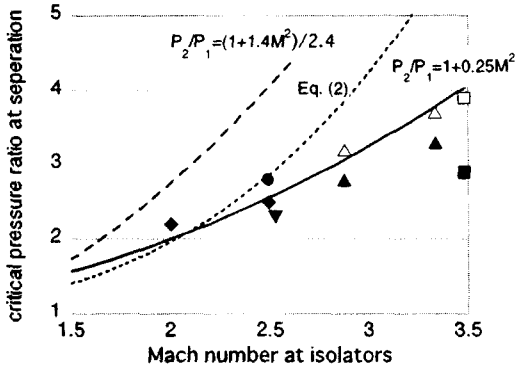

Figure 2 Relations between critical adverse pressure ratios and Mach numbers in engine tests from M4 to M8.

As a results, the M4 bleed area became 5130 mm². The porous plates has 533 holes, 3.5 mm in diameter (total hole area/bleed area: void ratio = 0.385). Harloff et al.[6] and Chu et al.[7] found a small discharge coefficient (Cd) of about 0.2 for their bleed holes from their numerical analysis. However, our discharge coefficient was measured to be 0.51 under the inlet condition. Due to the 30-mm-thick strut in the M6 engine, the bleed area was decreased to 2460 mm². A porous plate containing 196 holes with a diameter of 4 mm was

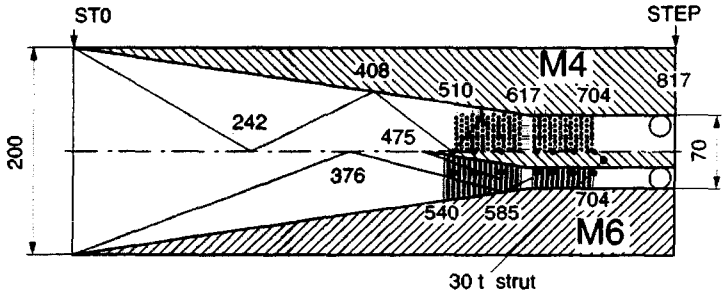

Figure 3 shockwave patterns and arrangements of porous plates for the M4 and M6 conditions

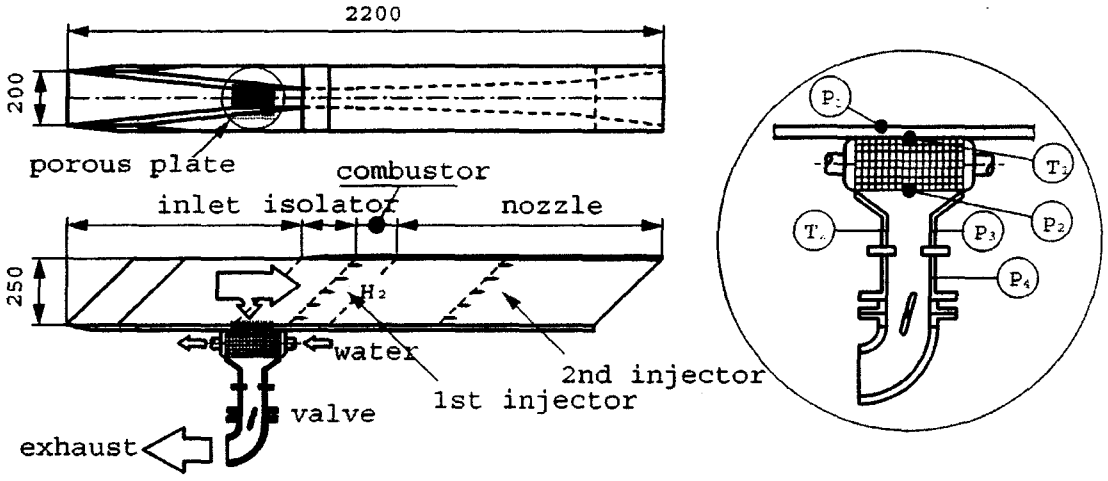

Figure 4 Scramjet engine with boundary layer bleed and two-staged injection of H_2.
The boundary layer bleed devise consists of a porous plate, an air cooler, a choked orifice and an ON/OFF valve.

designed for the small bleed area. The isolator pressure was also lower at 20 kPa in the M6 condition as compared with 40 kPa in the M4 case. Consequently, the maximum bleed rate in the M6 test was reduced to 30 g/s as compared with 200 g/s in the M4 case.

Air Coolers and Exhaust

Hot air with total temperatures of 870 K (M4) and 1500 K (M6) required air coolers in the bleed systems. The air coolers were installed downstream of the porous plates as illustrated in Fig. 4. The bleed rates of 200 g/s and 30 g/s corresponded to 3% (M4) and 0.6% (M6) of the total airflow rates in engines. The small suction rates enable the air cooler compactness for two reasons. Firstly, amounts of air to be cooled are small, secondly, the temperature of air bled is low because the bottom layer has already been cooled by the engine wall. Our coolers were designed to reduce the exhaust temperature to 400 K (M4 and M6) in the engine start condition, and to meet the requirement that the exhaust temperature should not exceed 650 K, even in the unstart condition.

The air bled through the porous plates is cooled in the plate. The M4 plate was uncooled and the M6 plate was water-cooled by 11 water passages. The air coolers were installed downstream of the porous plates. A radiator for air-conditioning in a compact car was utilized as the air cooler for the M4 bleed. The hydraulic diameter of the finned-tube radiator was 2.43 mm and the air passage length of 65 mm showed that the air temperature decreased to a level 0.3 times the initial difference in the temperature. The temperature of the exhaust from the cooler was estimated to be 480 K in the M4 condition. The M6 cooler (235 mm long, 95-mm wide and 55 mm high) was made of small kettle boilers. It was estimated that a hydraulic diameter of 6.1 mm would lower air temperature by 400 K in the cooler. Since the bled air in the M6 tests was pre-cooled in the water-cooled porous plate, we estimated that the exhaust temperature was reduced lower than 600 K.

The static pressure in engines was about 40 kPa (M4) to 20 kPa (M6). The bled air was autonomously exhausted to a test cell with a pressure of 12 kPa (M4) or 5 kPa (M6) after metering the bleed rates by the orifice (Cd = 0.93 by calibrations). In flight situations, the ambient pressure in spaceplanes is lower than these cell pressures. There is no difficulty in applying boundary layer bleed in flight engines. The bleed was controlled by an ON/OFF valve during combustion tests. The bleed rate was preset during the tests. Pressure, air and water temperatures are monitored at the locations indicated in Fig. 4.

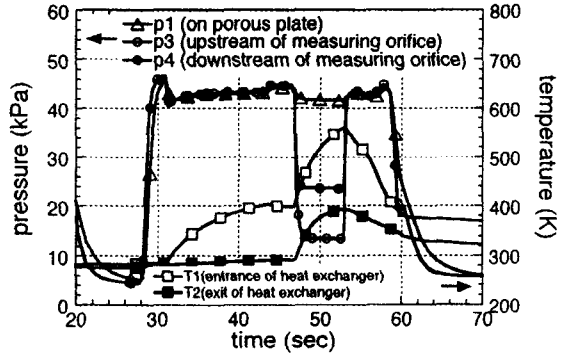

Figure 5 Variations of pressure and air temperature in the M4 bleed system.

Thrust Performance with BL Control

Mach 4 Tests

Figure 5 illustrates an example of measurement of static pressure and air temperature. The Mach 4 air condition is established at t = 31 sec and the wall pressure around the porous plate is indicated to be 43 kPa. The air temperature at the cooler raises from 300 K to 400 K because the hot air enters the bleed device. However, the temperature at the exhaust is unchanged because the bleed valve is closed. Pressures measured in the device indicate identical values of 43 kPa because there is no flow across the bleed device.

At t = 47 sec, the valve opens and the boundary layer bleed starts. The temperature in the device raises to 560 K and the exhaust temperature approach 400 K at t = 53 sec. The wall pressure measured on the porous plate decreases slightly from 43 kPa to 41 kPa during the bleed from 47 sec to 53 sec. The bleed rate is measured by the metering orifice. The solid circles denote the pressure upstream of the orifice and the open circles are the back pressure of the orifice. The metering orifice indicates a bleed air rate of 200 g/s. At t = 53 sec, the valve is closed. Bleed drag is measured by this ON/OFF operation of the bleed valve.

The requirement that the exhaust gas temperature should not exceed 600 K is satisfied. The most hostile condition to which the cooler is subjected is at the engine unstart, when the bleed device is subjected to combustion gas with a temperature of 2500 K. Our experiments showed that the highest gas temperature upstream of the cooler (downstream of the porous plate) was 630 K in the M4 tests.

Figure 6 shows the effects of boundary layer bleed on the wall pressure distributions in the M4 engines. The horizontal axis is the distance from the leading edge of the topwall. The wall pressure is normalized by using the total pressure of the M4 wind tunnel (860

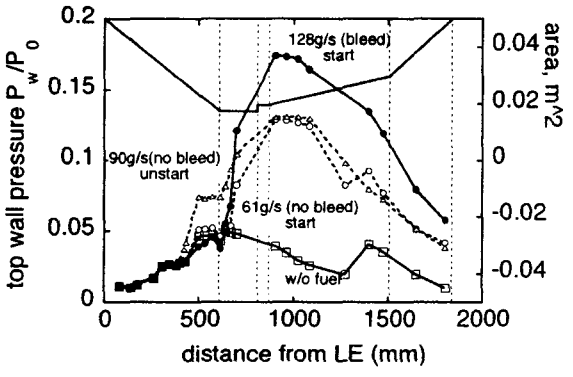

Figure 6 Effects of BL bleed (M4). A high pressure region b combustion of 128 g/s is anchored in the isolator.

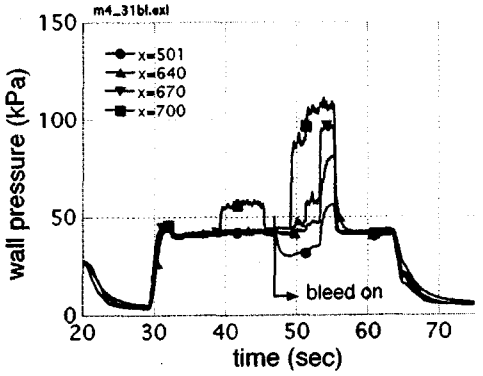

Figure 7 Wall pressures around the porous plate (M4)

kPa). The engine geometry is illustrated in the upper part of Fig. 6 in which the inlet, the isolator, the backward-facing step, the diverging combustor and the nozzle sections are shown by solid lines.

The wall pressure distribution before fuel supply is indicated by open squares in Fig. 6. The pressure increases to 0.05 at the combustor due to compression in the inlet. The high-pressure air expands through the diverging sections (x > 800 mm) toward the nozzle. A fuel supply rate of 61 g/s raises the wall pressure to 0.13P0 at the combustor and this increase of the wall pressure in the diverging sections produces thrust. The high pressure region is anchored in the isolator in the case of 61 g/s. Unfortunately, however, an increase of fuel rate to 90 g/s causes intrusion of the high pressure region into the inlet if boundary layer bleed is not applied. The intrusion of high pressure on the compression surface in the inlet increases drag and deteriorates thrust produced on the thrust surfaces. This is the engine unstart.

Effects of the bleed of 200 g/s are indicated by solid circles in the figure. The bleed reduces pressure on the porous plate around x = 600 mm. The most significant change is that the high pressure region is stabilized in the isolator even with a larger fuel rate of 128 g/s. Due to this stabilization, the maximum pressure reaches P =0.175P0 and the high pressure produces a greater thrust.

Time histories of wall pressures at several streamwise locations around the plate are shown in Fig. 7. The wind tunnel is activated at 31 sec and the engine drag under the fuel-off condition is measured at 32 sec < t < 38 sec. Two-stage injection is tested between 38 sec to 46 sec. Hydrogen is injected at a fixed rate of 49 g/s from the first injection orifice row and the rate of H2 from the second fuel orifice row is stepwisely increased to a maximum of 60 g/s during which no boundary bleed is applied. Although a sensor located at x = 700 mm (110 mm upstream of the step) indicates the combustion of the first-stage H2, no pressure changes are detected by other sensor located further upstream. This indicates that the high pressure region produced by the first-stage combustion is anchored at 670 mm < x < 700 mm in the isolator and that effects of the second-stage combustion do not propagate up to these sensor locations. The H2 injection rate of 109 g/s exceeds the H2 injection rate of 90 g/s resulting in the engine unstart in Fig. 6. This finding, that the second-stage combustion does not influence the flowfield in the isolator, implies that two-stage injection of fuel may function to retard engine unstart.

In Fig. 7, H2 supply is stopped at 46 sec and the bleed valve is opened at 47 sec. Suction of air through the porous plate decreases wall pressure at the uppermost location at x = 501 mm. However the effect diminishes downstream. Bleed drag of 120 N was measured during this stage. From 49 sec, H2 is injected only from the first H2 orifice row and the flow rate is increased step by step from 108 g/s to 128 g/s and to 146 g/s under the bleed ON condition. Note that the engine falls into the unstart condition at the H2 rate of 90 g/s if bleed is not applied. With increasing H2 injection rates, the influence gradually intrudes upstream. For instance, the high pressure region resulting from 108 g/s reaches x = 700 mm and combustion of 128 g/s is reflected by an increase in pressure to 60 kPa at x = 670 mm. However, the sensors upstream of 670 mm did not indicate any influence. When H2 is increased to a injection rate of 148 g/s, the high pressure region moves upstream across the porous plate and enters the inlet. The pressure in the inlet (x = 501 mm) jumps up to 60 kPa. and the pressure inside the bleed system increases to 56 kPa. This is the engine unstart in the M4 condition. Consequently, the thrust suddenly decreases from 2300 N to 1790 N. Thus, a small amount of

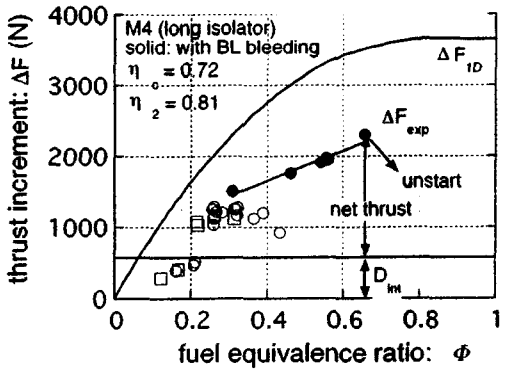

Figure 8 Doubled fuel rates and thrust by 3% -boundary layer bleed in Mach 4 condition

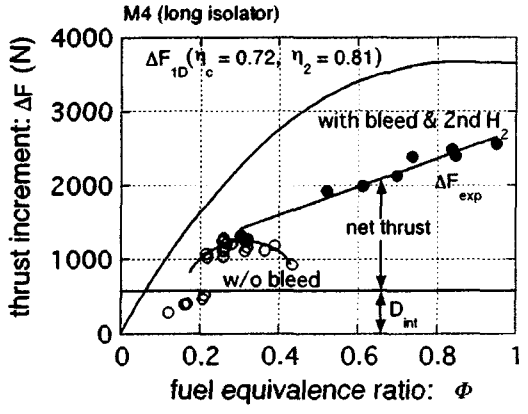

Figure 9 Tripled fuel rates and thrust by 3% bleed and two-staged combustion in Mach 4 condition

bleed in the inlet is effective in preventing engine unstart.

Figure 8 shows the effects of boundary layer controls on thrust increment (ΔF) by combustion in the M4 engine. The open symbols in Fig. 8 denote data obtained in the engine without bleed and the solid symbols are for the engine with boundary layer bleed. The solid line (ΔF_{ID}) denotes the theoretical maximum ΔF.[17] Comparison of ΔF_{ID} with ΔFexp yields achievement factors expressing combustion efficiencies and net thrust performances in our engine tests.[16] The combustion mode switches from a weak mode (flame blown-off to the downstream section) to an intense mode (flame anchored in the combustor) and causes a jump in ΔF from 500 N to 1000 N near Φ = 0.2. The engine without bleed shows a peak ΔF of 1200 N at Φ = 0.3 and the ΔF gradually diminishes in the region of $\Phi > 0.3$. This diminished ΔFexp is caused by the intrusion of high pressure into the inlet as discussed in Figs. 6 and 7. Since the internal drag (Dint) of the baseline engine was 570 N, the ΔFnet is 630 N and the Isp is 10.8 km/s in Table 1.

Improved thrust performance by the bleed of 3% (200 g/s) of the total air flow rate is illustrated by the solid symbols in Fig. 8. The engine operating range is now extended from Φ = 0.3 to Φ = 0.66 and the maximum ΔF doubles from 1200 N to 2300 N. Engine internal drag on the internal wet surface of engines was precisely measured by using subscale aerodynamic wind tunnels.[18] Bleed drag was measured by our engine test procedure and the engine internal drag was found to be Dint = 570 N without the bleed and 700 N with the bleed. Figure 8 illustrates that the engine net thrust increases from 630 N to 1400 N by the bleed. Thus, the small bleed rate of 3% doubles the engine operating range and thrust. The corresponding fuel specific impulse was 12.4 km/s at Φ0.66.

The secondary injection of H2 from the downstream section of engine yields further improvement in the thrust performance as shown in Fig. 9. Because combustion due to the second fuel injection does not strongly affect the flowfield in the isolator, the engine can operate up to Φ = 0.95 from Φ = 0.66 and the maximum ΔF increases from 2300 N to 2560 N. The ΔFnet becomes 1860 N and the Isp is found to be 10 km/s at Φ = 0.95 in Table 1.

Mach 6 Tests

Performance of the air-cooler used in the M6 engine is detailed in Fig. 10, where the upper half shows variations of pressure and the lower half shows the temperature histories. The Mach 6 wind tunnel is activated at 32 sec, at which point isolator pressure begins to increase. Mach 6 steady flow is established at 35 sec and the engine test is commenced. Since hot air with a total temperature of 1500 K fills the cavity in the bleed system, the temperature upstream of the air-cooler (behind the porous plate) increases gradually from 34 sec. The boundary layer bleed from 37 sec decreases the pressure downstream of the measuring orifice to the test cell pressure (4 kPa). The sensor

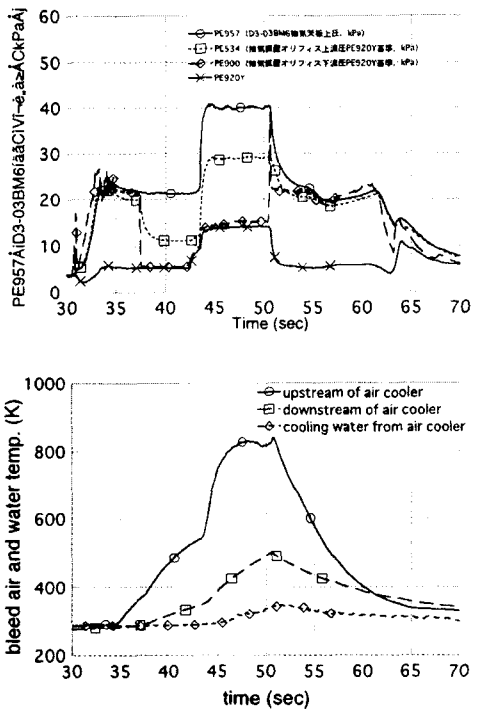

Figure 10 Performance of air-cooler in the M6 engine

upstream of the orifice indicates 12 kPa. The pressure difference across the orifice measures the bleed rate. Due to the hot air passing through the porous plate, the temperatures upstream and downstream of the cooler increase toward 550 K and 350 K, respectively. The saturated temperature found downstream of the cooler implies that the cooling performance is sufficient in the start condition.

With increasing H2 injection rate, the engine falls into the unstart condition at 42 sec and the unstart condition continues until 51 sec. This unstart causes "engine-test facility interference" and resulting in a rise of pressure around the bleed system as well as an increase of test cell pressure from 4 kPa to 14 kPa. The gas temperature downstream of the cooler increases toward 550 K and the temperature upstream of the cooler is saturated at 800 K. These results indicate

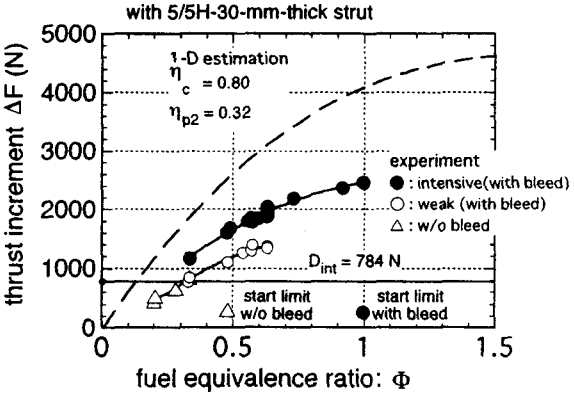

Figure 11 Doubled fuel rates and thrust by 0.6%- bleed (M6)

that the cooler functions well in the unstart condition. The engine restarts at 51 sec and the engine test is conducted till t = 60 sec.

Variation of the cooling water temperature is shown in the lower part of Fig. 10. The maximum increase of cooling water was found to be 50 K and heat balance between the cooled air and the heated water was confirmed.

The test data in the M6 condition is illustrated in Fig. 11. In these experiments, a 30-mm-thick strut is installed in the engine. The combustion mode switches from the weak mode to the intense mode and the thrust jumps near $\Phi = 0.3$. Above $\Phi = 0.3$, the engine operates in the intense combustion mode. When the boundary layer is not bled, the engine falls into unstart at $\Phi = 0.48$ just after attaining the maximum thrust of 1620 N (shown by the symbol X). Thus the limit fuel rate is found to be $\Phi = 0.48$ without the bleed.

Figure 11 shows that the bleed of 30 g/s (0.6% of captured air in the engine) extends the start limit from $\Phi = 0.48$ to $\Phi = 1$ to deliver a maximum thrust of 2460 N. By subtracting the Dint of 784 N, the ΔFnet is 1676 N and the fuel Isp is calculated to be 11.6 km/s as shown Table 1.

In the M4 tests, the two-staged injection of H_2 extended the engine start limit and increased the maximum thrust. However, it did not improve the thrust performance in the M6 condition. This is attributed to a limited residence time of fuel in the engine. Since the second injectors are located 462 mm upstream of the engine exit, the residence time of fuel injected from the second injectors is insufficient for the mixing and combustion. Studies on optimum injector locations in the multi-staged combustors for scramjet engines are required.

Conclusions

A boundary layer bleed system consisting of a porous plate, an air cooler, a metering orifices and an ON/OFF valve, was designed for each of our M4 and M6 engines. The bleed system was found to be effective in suppressing engine unstart transition. The following results were obtained in our engine tests under M4 and M6 conditions.

1) Bleed rates for suppressing boundary layer separation were analytically evaluated from comparison between the local dynamic pressure in the bottom layer and the critical adverse pressure to induce engine unstart.
2) Air coolers were optimized based on the bleed airflow rates. The exhaust air could be cooled below 600 K by cooling in the porous plates and the compact air coolers.
3) Our M4 engine tests showed that a small bleed rate of 3% doubled the engine operating range and the thrust in the M4 flight condition. With the assistance of two-staged injection of H2, the engine operating range was extended to $\Phi = 0.95$ and the maximum ΔF was further improved from 2300 N to 2560 N.
4) Our M6 tests showed that the bleed of 30 g/s (0.6% of captured air in the engine) extended the start limit from $\Phi = 0.48$ to $\Phi = 1$, resulting in delivery of a maximum thrust of 2460 N. However, the two-staged injection of fuel did not improve the thrust performance in the M6 condition, because the residence time of fuel injected from the second injectors was insufficient for mixing and combustion.

References

1. Chinzei, N., Mitani, T. and Yatsuyanagi, Y., "Scramjet Engine Research at the National Aerospace Laboratory in Japan," Scramjet Propulsion, edited by Curran, E. T. and Murthy, S. N. B., Vol. 189, Progress in Astronautics and Aeronautics, AIAA, New York, 2001, pp159-222.
2. Hiraiwa, T., Kanda, T., Kodera, M., Saito, T., Kobayashi, K., Kato, T., Effect of Induced Boundary Layer on Scramjet Engines' Thrust and Combustion Characteristics, AIAA 2003-4739, presented at 39th Joint Prop. Conf.,(2003).
3. Lachmann, G.,V. (Ed.), Boundary Layer and Flow Control, vols 1 &2, Pergaman Press, 1961
4. Fukuda, M. K., Hingst, W. R. and Eshotko, E., Bleed Effects on Shock/Boundary-Layer Interactions in Supersonice Mixed Compression Inlets, J. Aircraft, vol. 14, No. 2, pp151-156, 1977.
5. Syberg, J. and Koncsek, J. L., Bleed System Design Technology for Supersonic Inlets, J. Aircraft, vol 10, No. 7, pp407-413, 1973.
6. Harloff and, G. J. and Smith, G. E. , "On Supersonic-Inlet Boundary-Layer Bleed Flow," AIAA paper 95-0038, 1995.
7. Chyu, W. J. , "Effects of Bleed-Hole Geometry and Plenum Pressure on Three-dimensional Shockwave / Boundary Layer / Bleed Interactions," AIAA paper 93-3259, 1993.
8. Willis, B. P., Davis, D. O. and Hingst, W. R. , "Flow Coefficient Behavior for Boundary Layer Bleed Holes and Slots," AIAA paper 95-0031, 1995.
9. Tamayama, M, Sakata, K., Yanagi, R., Shindo, S., Murakami, A. and Honami, S., A Study of Three-Dimensional Interaction Flow Fields between Swept Shock Waves and Turbulent Boundary Layers, - Flow Structures and Effects of Bleed, National Aerospace Lab., TR 1227 (in Japanese), 1994.
10. Yanta, W. J., Collier, A.S., Spring III, W. C., Boyd, C. F., and McArthor, J. C., Experimental Measurements of the Flow in a Scramjet Inlet at Mach 4, J. Propulsion and Power, vol 6, No. 6, pp784-790, 1990.
11. Shimura, T. et al., M8 Simulation Tests on the Unstart Limit of a Scramjet Engine, ISTS 02-A-17, ISTS(2002)
12. K. Kobayashi, S. Tomioka, T. Hiraiwa, K. Kato, T. Kanda, and T. Mitani, "Suppression of Combustor-Inlet Interaction in a Scramjet Engine under M4 Flight Condition," AIAA 2003-4737, (2003).
13. Kodera, M., Tomioka, S., Kanda, T. and Mitani,

T., Mach 6 Test of a Scramjet Engine with Boundary-Layer Bleeding and Two-Staged Fuel Injection, AIAA 2003-7049, the 12th Spaceplane Conference, Norfolk, 2003.
14. Mitani, T., Tomioka, S., Kanda, T., Chinzei, N. and Kouchi, T., Scramjet Performance Achieved in Engine Tests from M4 to M8 Flight Conditions, AIAA 2003-7009, the 12th Space Plane Conf., Norfolk, 2003.
15. Holden, M. S., "Shock Wave -Turbulant Boundary Layer Interaction in Hypersonic Flow, AIAA paper 72-0074, 10th Aerospace Meeting, San Diego, January, 1972.
16. Korkegi, R.H., "A lower bound for three-dimensional turbulent separation in supersonic flow," AIAA J., vol. 23, No. 3, 1985, pp475-176.
17. Kouchi, T., Mitani, T., Hiraiwa, T., Tomioka, S., Masuya, G., Evaluation of Thrust Performance in Kinetic-Controlled Scramjet Engines with Measured Internal Drag, Journal of the Japan Society for Aeronautical and Space Science, vol. 51, No. 595, pp.403-411, 2003 (in Japanese).
18. Mitani, T., Izumikawa, M., Watanabe, S., Tarukawa, Y., Force Measurements of Fixied Geometry Scramjet Engines from Mach 4 to 8 Flight Condition, AIAA2002-5351, 2002.